Design and Synthesis of Malonic Acid-Based Inhibitors of Human Neutrophil Collagenase (MMP8)

Erich Graf von Roedern,[†,‡] Frank Grams,*,[§] Hans Brandstetter,[†,‖] and Luis Moroder*,[†]

*Max-Planck-Institut für Biochemie, D-82152 Martinsried, Germany, and Boehringer Mannheim,
Department Chemical Research, D-68305 Mannheim, Germany*

For most of the known synthetic inhibitors of matrix metalloproteinases (MMPs), a substrate-like binding mode was postulated on the basis of X-ray crystallographic structures of MMP/inhibitor complexes. Conversely, the malonic acid-based inhibitor (2*R,S*)-HONH-CO-CH(*i*-Bu)-CO-Ala-Gly-NH$_2$ was found to bind in a surprisingly different manner. Using this compound as a new lead structure, the interaction sites with human neutrophil collagenase (MMP8) were optimized with a series of iteratively designed analogues and with the help of X-ray structural analysis of selected inhibitors to finally produce low molecular weight nonpeptidic compounds of 500–1000-fold improved inhibitory potency.

Introduction

Matrix metalloproteinases (MMPs) are a family of zinc endopeptidases involved in tissue remodeling and thus in various disease processes including tumor invasion and joint destruction. Correspondingly, these enzymes represent attractive targets for inhibitor design and drug development.[1–5] Considerable insight into MMP–ligand interactions has been recently obtained from X-ray crystallography and NMR analysis,[6–19] and many new approaches to optimize MMP inhibitors have been guided by such structure-based knowledge. A central issue in this field is whether broad-spectrum MMP inhibitors or selective inhibitors targeted against individual MMP enzymes represent the most appropriate pharmacological strategy. This aspect is even more decisive if an enzyme or a group of enzymes can unequivocally be identified as the cause of a particular disease. Indeed it could be shown that certain MMP family members are coexpressed in higher amounts in certain diseases.[2]

Inspection of the known three-dimensional structures of MMPs shows that the S1′ pocket offers among the various subsites the greatest opportunity for a selective inhibitor design because there is considerable variation between the MMPs in the residues forming this substrate-binding subsite in the active-site cleft.

A large variety of more or less efficient MMP inhibitors including hydroxamic acids, phosphinic acids, thiols, etc. has been described,[1–5] and most of them contain a peptide-like moiety. The X-ray analyses of enzyme/inhibitor complexes, reported so far, revealed substrate-like binding modes of most of the inhibitors in extended conformations, whereas the malonic acid-based inhibitor (2*R,S*)-HONH-Mal(*i*-Bu)-Ala-Gly-NH$_2$ was found to bind in a nonsubstrate-like mode to human neutrophil collagenase (MMP8).[11] This type of inhibitors containing a malonic acid hydroxamate moiety has originally been designed for the metalloproteinase thermolysin[20] and was reported in early stages of the MMP inhibitor research.[21]

The binding mode of (2*R,S*)-HONH-Mal(*i*-Bu)-Ala-Gly-NH$_2$ to MMP8 is schematically outlined in Figure 1. The hydroxamate acts as bidentated chelator with each oxygen in optimal distance (2.2–2.3 Å) from the active-site Zn^{2+} ion. The hydrophobic substituent at the malonic acid moiety in the *S* configuration is pointing toward the edge strand of the enzyme active-site cleft. In contrast to the binding mode of the most potent inhibitors in clinical trials such as batimastat or marimastat which contain the succinic acid hydroxamate moiety,[15,22] in this malonic acid-based inhibitors there is no spacer between the chelating and the hydrophobic group. Correspondingly, the position of the side chain of the subsequent amino acid residue becomes similar, but not identical with that of P2′ residues of substrate-like binding inhibitors, while the residual peptidic tail is inserted into the S1′ pocket, thus leading to an overall β turn-like conformation of the inhibitor in the enzyme-bound state.

The discovery of this unique binding mode led us to explore the new lead structure in terms of stabilization of the bended conformation and modifications at the various interaction sites to improve the inhibitory potency of such malonic acid hydroxamate-based compounds.

Results and Discussion

Chemistry. The malonic acid-based inhibitors are composed of two parts, i.e., the malonic acid hydroxamate moiety and the residue R2 as shown in Figure 2. The R1-substituted diethyl malonates were prepared by standard procedures and then hydrolyzed with 1 equiv of KOH to produce the malonate monoethyl esters which
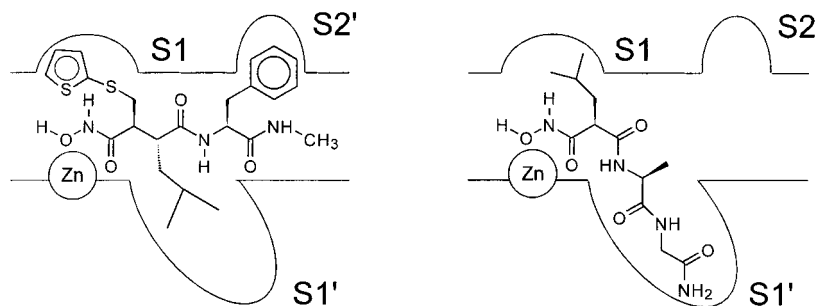
Figure 1. Schematic presentation of the substrate-like binding mode of batimastat (left)[15] and the nonsubstrate-like binding mode of HONH-Mal(*i*-Bu)-Ala-Gly-NH$_2$ (**8**) (right)[11] to MMP8.
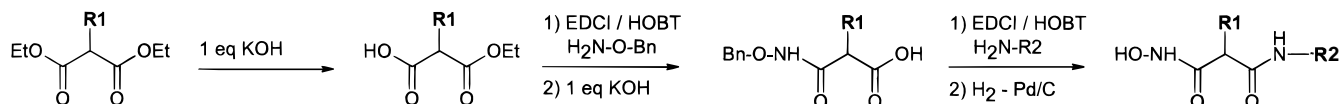

Figure 2. General scheme of synthesis used for the preparation of the malonic acid hydroxamates.

were condensed with (benzyloxy)amine following essentially known procedures.[23-25] With the use of EDCI/HOBT as coupling reagent, the guanidine adduct as observed with the DCC/HOBt method[23] was formed to negligible extents, and because of its water solubility, it was easily separated together with the resulting urea from the *N*-(benzyloxy)malonamic acid ethyl esters. After an additional saponification step with excesses NaOH, the resulting benzyl-protected malonic acid hydroxamates were amidated with the R2-NH$_2$ moieties consisting of amino acid derivatives or aryl- and alkyl-amines again by the EDCI/HOBt procedure. Finally, acidolytic removal of side-chain protecting groups, when required, followed by hydrogenolytic cleavage of the benzyl group from the hydroxamate over Pd/C catalyst gave the target hydroxamic acids. Performing the hydrogenolysis at a low stream of hydrogen and monitoring the product formation, reduction of the hydroxamic acids to the amide[23] was largely suppressed. Among all compounds only HONH-Mal(*i*-Bu)-Asp-NHBn (**12b**) was obtained as a pure diastereomer by crystallization of the protected precursor from ether. There is strong support for the *S* configuration of the 2-isobutylmalonic acid residue of this diastereomer, since it is a more potent inhibitor than the diastereomeric mixture **12**, and in crystals of the complexes **8**/MMP8[11] and **17**/MMP8,[26] the enzyme-bound malonic acid moiety is unequivocally in the *S*-configuration, whereas in crystals of the **12**/MMP8 complex[26] an unambiguous assignment of the configuration was not possible. For the remaining compounds, the composition of the diastereomeric ratios was determined by ^{1}H NMR spectroscopy.

Peptidic Malonic Acid-Based Inhibitors. Using the binding mode of (2*R*,*S*)-HOHN-Mal(*i*-Bu)-Ala-Gly-NH$_2$ (**8**) as lead structure, positions A−D outlined in Figure 3 were the targets of our attempts to optimize the inhibition of MMP8 by such malonic acid-based hydroxamic acids.

Modifications in Positions A and B of the Lead Structure. Replacement of the Gly-NH$_2$ tail of **8** with the more hydrophobic benzylamide led to improvement of the inhibitory potency by a factor of about 3−4 (Table 1). Therefore, in a first series of malonic acid hydroxamates benzylamide derivatives were synthesized with replacements of the Ala residue for exploring the
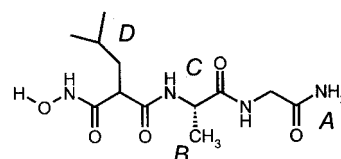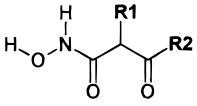

Figure 3. Positions A−D of the lead structure HONH-Mal-(*i*-Bu)-Ala-Gly-NH$_2$ (**8**) were the synthetic targets in the present study for improving inhibition of MMP8 by malonic acid hydroxamates.

Table 1. Inhibition of MMP8 with Peptidic Malonic Acid-Based Hydroxamates

	Compound	Diastereomeric Ratio	K_i [µM]
(structure) Ala–Gly–NH$_2$	**8**	36:64	121
XXX:			
Ala	**9**	40:60	50
D-Ala	**10**	25:75	194
Ser	**11**	28:72	35
Asp	**12**	43:57	136
Asp	**12b**	100: 0	88
Asn	**13**	34:66	55
Pro	**14**	50:50	168
Abz	**15**	50:50	36
Phe	**16**	37:63	25
(structure) Asn-N...NH$_2$	**17**	44:56	26

R1:	R3:			
i-Butyl	CH$_3$	**18**	23:77	1.4
i-Butyl	OH	**19**	24:76	12
i-Butyl	COOCH$_3$	**20**	22:78	9.6
i-Butyl	COOH	**21**	50:50	20
CH$_2$-Ph	CH$_3$	**22**	43:57	1.7
(CH$_2$)$_2$-Ph	CH$_3$	**23**	25:75	4.0
OH	CH$_3$	**24**	45:55	1.6

position B of Figure 3. The side chain of Ala in the **8**/MMP8 complex is pointing toward the S2′ subsite of the enzyme without apparent interactions. A change of the chirality of the Ala residue (**10**) was found to completely reverse the beneficial effects of the hydrophobic tail leading to a K_i value identical with that of just the malonic acid moiety, i.e., of (2*R*,*S*)-HOHN-Mal-

Table 2. Inhibition of MMP8 with Nonpeptidic Malonic Acid Hydroxamates

$$H-O-\overset{H}{\underset{}{N}}-\overset{O}{\underset{}{C}}-\overset{R1}{\underset{}{CH}}-\overset{O}{\underset{}{C}}-R2$$

R1	R2	compd	K_i (μM)
isobutyl	O-ethyl	**25**	190
Ph	O-ethyl	**26**	98
CH₂Ph	O-ethyl	**27**	53
(CH₂)₂Ph	O-ethyl	**28**	189
CH₂Ph	*N*-morpholide	**29**	50
CH₂Ph	NHCH₂Ph	**30**	3.1
(CH₂)₂Ph	NHCH₂Ph	**31**	2.3
isobutyl	NH(CH₂)₃Ph	**32**	0.54
CH₂Ph	NH(CH₂)₃Ph	**33**	0.56
(CH₂)₂Ph	NH(CH₂)₃Ph	**34**	0.49
OH	NH(CH₂)₃Ph	**35**	2.3
isobutyl	NH-*n*-octyl	**36**	0.24

(*i*-Bu)-OEt (**25**) (Table 2). Correspondingly, in all subsequent modifications the L-configuration was retained for this residue, and Ala was replaced by the amino acids Ser (**11**), Asp (**12**), and Asn (**13**), which according to modeling experiments were expected to form hydrogen-bonding networks with Tyr219N and Glu158O of the active-site cleft of MMP8. Although the X-ray structure of the **12**/MMP8 complex[26] revealed that additional hydrogen bonds were indeed formed as listed in Table 3, a significant improvement in the inhibitory potency was not achieved. This can only be explained if the favored binding energy is attenuated by opposite effects, e.g., by the strong solvation of these hydrophilic side chain. However, by incorporating into the Asn analogue **13** an amino group at the meta position of benzylamide as potential hydrogen-bonding donor a 2-fold enhanced inhibition of the enzyme by compound **17** in comparison to **13** was obtained. In fact, the X-ray structure of the **17**/MMP complex[26] revealed that this amino group in the crystal is located in hydrogen-bonding distance to Glu158CO and Leu193CO, as shown in Table 3 in comparison to other inhibitors.

Conformational Restraints in Position C of the Lead Structure. To possibly stabilize the bended structure of these malonic acid-based inhibitors, the Ala residue in compound **8** was replaced with the conformationally restrained residues Pro (**14**) and the β-amino acid 2-aminobenzoic acid (Abz) (**15**), however, without achieving significant improvements of the inhibitory potency (Table 1). Nevertheless, the K_i value of compound **15** clearly indicated that the hydrophobic character of the S2′ subsite could represent a promising interaction site. Correspondingly, the Phe analogue **16** was synthesized which exhibited almost the identical K_i value as that of the Abz analogue **15**. Increased hydrophobic interactions both in the S1′ and S2′ subsites were attempted with the *h*Phe analogue **18** where the C-terminal tail was further extended, i.e., as [2-(4-methyl)phenyl]ethyl amide derivative, as suggested by modeling experiments. Indeed a significant improvement was obtained with a K_i of 1.4 μM that suggests additional hydrophobic interactions of the *h*Phe side chain with the S2′ subsite and a good fit of the tail into the S1′ pocket. Further attempts to improve the binding affinities of the *h*Phe analogue **18** by introduction of hydrophilic moieties in the para position of the 2-phenylethyl group, like the hydroxyl (**19**), carboxyl (**21**), or

methyl ester function (**20**), to possibly favor hydrogen bond or salt bridge interactions with the Arg222 residue on the bottom of the S1′ pocket, was not achieved as evidenced by the 10−20-fold reduced inhibitory potencies.

Modifications in Position D. In the **8**/MMP8 X-ray structure the isobutyl group is occupying the S1 subsite of the enzyme in an hydrophobic surface-type interaction.[11] Since omission of the isobutyl group in the Asp derivative **12** led to a 10-fold increase of the K_i to about 1 mM, we have replaced the isobutyl moiety in compound **18** with the benzyl or 2-phenylethyl group (compounds **22** and **23**); both compounds showed a reduced inhibition of MMP8 (Table 1). On the other hand, by substituting the hydrophobic isobutyl group in **18** with an hydroxyl function (**24**), practically no effect on the inhibitory potency was observed.

Nonpeptidic Malonic Acid-Based Inhibitors. In the first series of MMP8 inhibitors **8**−**24** the pseudo P1 residue is linked to the pseudo P1′ residue via a three- and four-atom (compound **15**) spacer formed by an α- or β-amino acid residue. The results obtained with the differently C2-substituted malonic acid derivatives **25**−**28** (Table 2) were compelling to attempt direct linkage of the P1 and P1′ groups. Correspondingly, the malonic acid derivatives **27** and **28** were converted to the morpholide and benzylamides. While with the morpholide **29** no improvement in the K_i values was observed, the benzylamides **30** and **31** were found to exhibit inhibitory potencies comparable to those of the best peptidic inhibitors with K_i values of 3.1 and 2.3 μM, respectively (Table 2).

To allow for deeper insertion of the C-terminal aromatic group into the S1′ subsite, the benzyl group was replaced by the 3-phenylpropyl group. The related derivatives of the 2-isobutyl- (**32**), 2-benzyl- (**33**), and 2-(2-phenylethyl)- (**34**) malonic acid hydroxamates showed very similar K_i values of about 0.5 μM which were therefore independent of the P1 mimetic group as long as hydrophobic interactions at the S1 subsite were retained. By canceling these interactions, e.g., with the hydroxyl derivative **35**, again a 4−5-fold lower affinity for MMP8 was measured. Finally, mimicking the total number of backbone atoms of the peptidic inhibitors with an aliphatic C8 amide substituent (**36**) a further decrease of the K_i to 0.24 M was obtained, suggesting a certain degree of flexibility for the substituents as an important feature for optimal occupancy of the deep hydrophobic S1′ subsite of MMP8.

To conclude, taking advantage of the information gained with the X-ray structures of a few selected hydroxamate inhibitors on malonic acid basis, about 500-fold improved inhibition of MMP8 to submicromolar K_i values could be achieved in comparison to the lead structure **8** by stepwise optimization of the interaction sites and finally conversion of the peptidic structures into low molecular weight nonpeptidic malonic acid derivatives.

Experimental Section

Materials and Methods. The amino acid derivatives used in the synthesis were prepared according to standard procedures.[27] Solvents and reagents were of the highest quality commercially available. Dnp-Pro-Leu-Gly-Leu-Trp-Ala-D-Arg-NH₂ was purchased from Bachem (Heidelberg, Germany). TLC

Table 3. Hydrogen Bond Interactions of the MMP8 Active Site with the Inhibitors Batimastat,[15] HONH-Mal(*i*-Bu)-Ala-Gly-NH$_2$ (**8**),[11] HONH-Mal(*i*-Bu)-Asp-NHBzl (**12**),[26] and HONH-Mal(*i*-Bu)-Asn-NHBzl-(*m*-NH$_2$) (**17**)[26]

batimastat		HONH-Mal(*i*-Bu)-Ala-Gly-NH$_2$ (**8**)		HONH-Mal(*i*-Bu)-Asp-NHBn (**12**)		HONH-Mal(*i*-Bu)-Asn-NHBn-(*m*-NH$_2$) (**17**)	
OH(NHOH)-Glu198O	2.9/2.4 Å	OH(NHOH)-Glu198Oε1/2	3.1/3.2 Å	OH(NHOH)-Glu198O	2.9/2.8 Å	OH(NHOH)-Glu198O	2.5/3.1 Å
NH(NHOH)-Ala161O	3.0 Å	NH(NHOH)-Ala161O	2.9 Å	NH(NHOH)-Ala161O	3.1 Å	NH(NHOH)-Ala161O	2.8 Å
O(I1)-Leu160N	2.8 Å	O(I1)-Leu160N	2.7 Å	O(I1)-Leu160N	3.0 Å	O(I1)-Leu160N	2.7 Å
N(I2)-Pro217O	3.3 Å	O(I1)-Ala161N	3.5 Å	O(I1)-Ala161N	3.4 Å	O(I1)-Ala161N	3.4 Å
O(I2)-Tyr219N	3.0 Å			Oδ1(I2)-Tyr219N	3.0 Å	Oδ1(I2)-Tyr219N	3.0 Å
N1(I2)-Gly158O	3.1 Å			Nδ2(I2)-Glu158O	2.9 Å	Nδ2(I2)-Glu158O	2.9 Å
				O(I2)-Tyr219N	3.1 Å	O(I2)-Tyr219N	3.4 Å
				Oδ2(I2)-Gly158O	3.0 Å	Oδ2(I2)-Gly158O	

silica gel 60 plates were from Merck AG (Darmstadt, Germany), and compounds were visualized with the chlorine/tolidine or permanganate reagent. FAB-MS spectra were recorded on a Finnigan MAT 900 and the NMR spectra on AMX 400 and AMX 500 (Bruker).

Enzyme Assay. The catalytic domain of MMP8 (Phe[79], Gly[242]-MMP8) was used for the inhibition experiments. Enzyme assays were performed at 25 °C in 10 mM CaCl$_2$, 100 mM NaCl, 50 mM Tris/HCl (pH 7.6) using 8 nM enzyme concentration and the fluorogenic substrate Dnp-Pro-Leu-Gly-Leu-Trp-Ala-D-Arg-NH$_2$ (1 × 10^{-5} M). Enzyme kinetics were performed essentially as described by Stack et al.,[28] and the increase in fluorescence at 350 nm was monitored over a period of 100 s with a luminescence spectrometer LS 50B (Perkin-Elmer) to determine initial rates of hydrolysis. Evaluation of the kinetic data was performed as reported by Copeland et al.[29] Assuming Michaelis–Menten kinetics, the K_i values were then calculated with the program Enzfitter (Version 1.05, 1987, Elsevier-Biosoft).

Computational Methods. Docking calculations were performed on the crystal structure of MMP8[11] using the program package INSIGHT/DISCOVER (version 2.96, MSI Technologies, San Diego, CA). By keeping the protein structure fixed and the hydroxamate function as ligand of the active-site Zn^{2+} as determined in the **8**/MMP8 complex as constraint, alternative orientations and conformations of potential new inhibitors were generated and energy-minimized to convergence. For inspection of the possible binding mode of newly designed ligands, interaction sites have been generated with the program LUDI.[30]

Synthesis: (2*R,S*)-BnONH-Mal(*i*-Bu)-OH (2). To a suspension of (benzyloxy)amine hydrochloride (4.79 g, 30 mmol) in THF was added sodium methylate (1.62 g; 30 mmol) under stirring, and after 10 min the solvent was evaporated. The residue was resuspended in THF and reacted at 0 °C with (2*R,S*)-EtO-Mal(*i*-Bu)-OK[23] (6.78 g, 30 mmol), EDCI (6.34 g, 33 mmol), and HOBt (4.6 g, 33 mmol). The reaction mixture was allowed to reach room temperature, and after 12 h it was worked up by washing the crude product in AcOEt with 5% KHSO$_4$, 5% NaHCO$_3$, and water. The organic layer was dried over MgSO$_4$ and evaporated; yield of (2*R,S*)-BnONH-Mal(*i*-Bu)-OEt (**1**): 7.45 g (84.6%); colorless oil; TLC (AcOEt/*n*-hexane, 1:2) R_f 0.3.

Compound **1** (3.53 g, 12 mmol) was saponified in THF/MeOH (1:1) with NaOH (1.44 g, 36 mmol) in 2 mL of water at 50 °C for 1 h. The reaction mixture was diluted with MeOH and treated with 10 g of amberlyst 15 (H$^+$ form; 4.6 mmol/g) under ice cooling. The resin was filtered off and washed with MeOH, and the combined filtrates were evaporated to dryness: yield 3.2 g (85%), needles; TLC (CH$_3$CN/H$_2$O, 4:1) R_f 0.6; FAB-MS *m/z* 266.1 [M + H$^+$]; M_r = 265.1 calcd for C$_{14}$H$_{19}$NO$_4$; ^{1}H NMR (DMSO-d_6) δ 11.26 (s, 1H, N*H*OBn), 7.34–7.39 (m, 5H, C$_6$H$_5$), 4.78 (s, 2H, CH$_2$ (Bn)), 3.03 (dd, 1H, H-C2 (Mal)), 1.37–1.65 (m, 3H, H-C3 (Mal) + H-C4 (Mal)), 0.85 (2 d, 6H, 2 CH$_3$); the analytical data are consistent with those reported by Bihovsky et al.[23]

(2*R,S*)-BnONH-Mal(Bn)-OH (4). (2*R,S*)-EtO-Mal(Bn)-OK was converted to (2*R,S*)-BnONH-Mal(Bn)-OEt (**3**) as described for compound **1**: yield 88%; TLC (AcOEt/*n*-hexane, 1:1) R_f 0.4; ^{1}H NMR (DMSO-d_6) the spectrum is consistent with the structure. Compound **3** was saponified and worked up as

described for **2**: yield 95%; the analytical data were consistent with those reported by Fournie-Zaluski et al.[24]

(2*R,S*)-BnONH-Mal(CH$_2$CH$_2$Ph)-OH (6). (2*R,S*)-BnONH-Mal(CH$_2$-CH$_2$-Ph)-OEt (**5**) was obtained from (2*R,S*)-EtO-Mal-(CH$_2$-CH$_2$-Ph)-OH[31] as described for **1**: yield 55%; TLC (AcOEt/*n*-hexane, 1:1) R_f 0.4; FAB-MS *m/z* 342.2 [M + H$^+$]; M_r = 341.19 calcd for C$_{20}$H$_{23}$NO$_4$; ^{1}H NMR (DMSO-d_6) the spectrum is consistent with the structure. Compound **5** was saponified to **6**: yield 96%; TLC (CH$_3$CN/H$_2$O, 4:1) R_f 0.65; ^{1}H NMR (DMSO-d_6) δ 13.2 (s (br), 1H, COOH), 11.32 (s, 1H, NH), 7.3–7.4 (m, 10H, 2 C$_6$H$_5$), 3.09 (t, 1H, H-C2 (Mal)), 2.50 (t, 2H, H-C4 (Mal)), 2.02 (m, 2H, H-C3 (Mal)).

(2*R,S*)-BnONH-Mal(OBn)-OH (7). EtO-Mal(OBn)-OEt[32] was converted to the title compound as described for **2**: yield 58% over the two steps; colorless powder; TLC (CH$_3$CN/H$_2$O, 4:1) R_f 0.25; ^{1}H NMR (DMSO-d_6) δ 13.1 (s (br), 1H, COOH), 11.50 (s, 1H, NH), 7.3–7.4 (m, 10H, 2 C$_6$H$_5$), 4.83 (s, 2H, CH$_2$ (BnONH)), 4.53 (2 d, 2H, CH$_2$ (OBn)), 4.34 (s, 1H, H-C2 (Mal)).

(2*R,S*)-HONH-Mal(*i*-Bu)-Ala-Gly-NH$_2$ (8). The compound was prepared from **2** and H-Ala-Gly-NH$_2$ as described for **9**. The analytical data were consistent with those reported by by Nishino and Powers;[25] diastereomeric ratio was 36:64.

(2*R,S*)-HONH-Mal(*i*-Bu)-Ala-NHBn (9). To H-Ala-NH-Bn[33] (0.18 g, 1.0 mmol) in THF at 0 °C were added compound **2** (0.27 g, 1.0 mmol), HOBt (0.14 g, 1.0 mmol), and EDCI (0.20 g, 1.05 mmol). The reaction mixture was stirred for 12 h, allowing room temperature to be reached. The solvent was then evaporated and the residue distributed between AcOEt and water. The organic phase was washed with 5% KHSO$_4$, 5% NaHCO$_3$, and water, dried over MgSO$_4$, and evaporated to small volume. The product was precipitated with ether and then hydrogenated in MeOH over 10% Pd/C catalyst for 1 h. The catalyst was filtered off, the filtrate was evaporated to small volume, and the product was precipitated with ether: yield 187 mg (56%); TLC (CHCl$_3$/MeOH, 9:1) R_f 0.4; FAB-MS *m/z* 336.4 [M + H$^+$]; M_r = 335.41 calcd for C$_{17}$H$_{25}$N$_3$O$_4$; ^{1}H NMR (DMSO-d_6) δ 10.57 + 10.51 (2 s, 1H, N*H*OH), 8.97 (s, 1H, OH), 8.44–8.52 (m, 1H, NHBn), 7.84 + 7.94 (2 d, 1H, NH (Ala)), 7.20–7.39 (m, 5H, C$_6$H$_5$), 4.30 (m, 3H, Hα (Ala) + CH$_2$ (Bn)), 3.00–3.10 (m, 1H, H-C2 (Mal)), 1.37–1.65 (m, 3H, H-C3 (Mal) + H-C4 (Mal)), 1.27 (d, 3H, CH$_3$ (Ala)), 0.85 (2 d, 6H, 2 CH$_3$); diastereomeric ratio, 40:60.

The following HONH-Mal(*i*-Bu)-Xxx-NHBn analogues were prepared by identical procedures via coupling of the malonic acid derivative **2** with H-Xxx-NHBn using the EDCI/HOBt procedure followed by deprotection via hydrogenolysis over 10% Pd/C.

(2*R,S*)-HONH-Mal(*i*-Bu)-D-Ala-NHBn (10): yield 50% over the two steps; TLC (CHCl$_3$/MeOH, 9:1) R_f 0.4; FAB-MS *m/z* 336.4 [M + H$^+$]; M_r = 335.41 calcd for C$_{17}$H$_{25}$N$_3$O$_4$; ^{1}H NMR (DMSO-d_6) δ 10.57 + 10.51 (2 s, 1H, N*H*OH), 8.97 (br, 1H, OH), 8.44–8.52 (m, 1H, NHBn), 7.84 + 7.94 (2 d, 1H, NH (Ala)), 7.20–7.39 (m, 5H, C$_6$H$_5$), 4.30 (m, 3H, Hα (Ala) + CH$_2$ (Bn)), 3.00–3.10 (m, 1H, H-C2 (Mal)), 1.37–1.65 (m, 3H, H-C3 (Mal) + H-C4 (Mal)), 1.27 (d, 3H, CH$_3$ (Ala)), 0.85 (d, 6H, 2 CH$_3$); diastereomeric ratio, 25:75.

(2*R,S*)-HONH-Mal(*i*-Bu)-Ser-NHBn (11): yield 78% over the two steps; TLC (CHCl$_3$/MeOH, 9:1) R_f 0.2; FAB-MS *m/z* 352.2 [M + H$^+$]; M_r = 351.18 calcd for C$_{17}$H$_{25}$N$_3$O$_5$; ^{1}H NMR (DMSO-d_6) δ 10.50 (br, 1H, N*H*OH), 9.00 (br, 1H, OH), 8.45–8.56 (m, 1H, NHBn), 7.80 + 7.96 (2 d, 1H, NH (Ser)), 7.20–

7.39 (m, 5H, C$_6$H$_5$), 5.00 (br, 1H, OH (Ser)), 4.30 (m, 3H, Hα (Ser) + CH$_2$ (Bn)), 3.55 + 3.65 (2 ddd, 2H, CH$_2$ (Ser)), 3.00–3.10 (m, 1H, H-C2 (Mal)), 1.37–1.65 (m, 3H, H-C3 (Mal) + H-C4 (Mal)), 0.85 (d, 6H, 2 CH$_3$); diastereomeric ratio, 28:72.

(2R,S)-HONH-Mal(i-Bu)-Asp-NHBn (12). Prior to the hydrogenation step, exposure to TFA (1 h) was used to deprotect the Asp(OtBu) residue: yield 70% over the three steps; TLC (CH$_3$CN/H$_2$O, 4:1) R_f 0.55; FAB-MS m/z 380.2 [M + H$^+$]; M_r = 379.18 calcd for C$_{18}$H$_{25}$N$_3$O$_6$; ^{1}H NMR (DMSO-d_6) δ 10.52 (s, 1H, NHOH), 9.00 (br, 1H, OH), 8.35–8.45 (m, 1H, NHBn), 8.05 + 8.13 (2 d, 1H, NH (Asp)), 7.20–7.35 (m, 5H, C$_6$H$_5$), 4.60 (m, 1H, Hα (Asp)), 4,30 (m, 2H, CH$_2$ (Bn)), 3.00–3.15 (m, 1H, H-C2 (Mal)), 2.58 + 2.69 (2 dd, 2H, CH$_2$ (Asp)), 1.40–1.65 (m, 3H, H-C3 (Mal) + H-C4 (Mal)), 0.85 (d, 6H, 2 CH$_3$); diastereomeric ratio, 43:57. One pure diastereomer (**12b**) could be isolated by crystallization of the protected precursor (2R,S)-BnONH-Mal(i-Bu)-Asp(OtBu)-NHBn from ether.

(2R,S)-HONH-Mal(i-Bu)-Asn-NHBn (13): yield 59% over the two steps; TLC (CH$_3$CN/H$_2$O, 4:1) R_f 0.6; FAB-MS m/z 379.2 [M + H$^+$]; M_r = 378.18 calcd for C$_{18}$H$_{26}$N$_4$O$_5$; ^{1}H NMR (DMSO-d_6) δ 8.42–8.55 (m, 1H, NHBn), 8.20 (m, 1H, NH (Asn)), 7.45 + 6.88 (2 s, 2H, NH$_2$ (Asn)), 7.15–7.35 (m, 5H, C$_6$H$_5$), 4.57 (m, 1H, Hα (Asn)), 4,25 (m, 2H, CH$_2$ (Bn)), 3.05–3.15 (m, 1H, H-C2 (Mal)), 2.50 (m, 2H, CH$_2$ (Asn)), 1.40–1.65 (m, 3H, H-C3 (Mal) + H-C4 (Mal)), 0.85 (d, 6H, 2 CH$_3$); diastereomeric ratio, 34:66.

(2R,S)-HONH-Mal(i-Bu)-Pro-NHBn (14): yield 22% over the two steps; TLC (CHCl$_3$/MeOH, 9:1) R_f 0.3 and 0.4 for the two diastereoisomers; FAB-MS m/z 362.3 [M + H$^+$]; M_r = 361.18 calcd for C$_{19}$H$_{27}$N$_3$O$_4$; ^{1}H NMR (DMSO-d_6) δ 10.60 + 10.65 (2 s, 1H, NHOH), 8.90 + 8.96 (2 s, 1H, OH), 8.30 (m, 1H, NHBn), 7.20–7.35 (m, 5H, C$_6$H$_5$), 4.20–4.35 (m, 3H, Hα (Pro), CH$_2$ (Bn)), 3.50–3.70 (m, 2H, Hδ (Pro)), 3.35 (m, 1H, H-C2 (Mal)), 1.4–2.2 (m, 7H, Hβ (Pro)), Hγ (Pro)), H-C3 (Mal), H-C4 (Mal)), 0.90 (m, 6H, 2 CH$_3$); diastereomeric ratio, 50:50.

(2R,S)-HONH-Mal(i-Bu)-Abz-NHBn (15): yield 40% over the two steps; FAB-MS m/z 384.1 [M + H$^+$]; M_r = 385.18 calcd for C$_{21}$H$_{25}$N$_3$O$_4$; ^{1}H NMR (DMSO-d_6) δ 11.28 (s, 1H, NH(Abz)), 10.77 (2 s, 1H, NHOH), 8.96 (s, 1H, OH), 9.25 (m, 1H, NHBn), 8.35 (d, 1H, aryl (Abz)), 7.77 (d, 1H, aryl (Abz)), 7.48 (dd, 1H, aryl (Abz)), 7.15 (dd, 1H, aryl (Abz)), 7.20–7.35 (m, 5H, C$_6$H$_5$), 4.50 (m, 2H, CH$_2$ (Bn)), 3.17 (dd, 1H, H-C2 (Mal)), 1.4–1.75 (m, 3H, H-C3 (Mal), H-C4 (Mal)), 0.87 (d, 6H, 2 CH$_3$); racemic mixture.

(2R,S)-HONH-Mal(i-Bu)-Phe-NHBn (16): yield 80% over the two steps; TLC (CHCl$_3$/MeOH, 9:1) R_f 0.4; FAB-MS m/z 412.2 [M + H$^+$]; M_r = 411.21 calcd for C$_{23}$H$_{29}$N$_3$O$_4$; ^{1}H NMR (DMSO-d_6) δ 10.45 (s, 1H, NHOH), 8.92 (s, 1H, OH), 8.56 (m, 1H, NHBn), 7.85 + 8.03 (2 d, 1H, NH (Phe)), 7.20–7.39 (m, 10H, 2 C$_6$H$_5$), 4.57 (m, 1H, Hα (Phe), 4,30 (m, 1H, CH$_2$ (Bn)), 2.75–3.10 (m, 3H, CH$_2$ (Phe), H-C2 (Mal)), 1.20–1.50 (m, 3H, H-C3 (Mal) + H-C4 (Mal)), 0.75 (m, 6H, 2 CH$_3$); diastereoisomeric ratio, 37:63.

(2R,S)-HONH-Mal(i-Bu)-Asn-NHBn-(m-NH$_2$) (17). 3-Nitrobenzylamine was reacted with Boc-Asn-ONp and worked up by standard procedures: yield 63%; TLC (CHCl$_3$/MeOH, 9:1) R_f 0.35; mp 190–191 °C. Boc-Asn-NHBn-(m-NO$_2$) was deprotected with 4 N HCl in dioxane. The solution was concentrated to a small volume, and H-Asn-NHBn-(m-NO$_2$)·HCl was precipitated with ether and then coupled with the malonic acid derivative **2** by the EDCI/HOBt procedure in the presence of triethylamine as auxiliary base. The reaction mixture was worked up as described for **9**: yield 40%; TLC (CHCl$_3$/MeOH, 9:1) R_f 0.3; ^{1}H NMR (DMSO-d_6) the spectrum is consistent with the assigned structure.

(2R,S)-BnONH-Mal(i-Bu)-Asn-NHBn-(m-NO$_2$) was hydrogenated in MeOH in the presence of equivalent amounts of 1 N HCl over 10% Pd/C catalyst for 10 h. The catalyst was filtered off, and the filtrate was concentrated to a small volume. The product was precipitated with ether: yield 92%; TLC (CHCl$_3$/MeOH, 4:1) R_f 0.15; FAB-MS m/z 394.2 [M + H$^+$]; M_r = 393.20 calcd for C$_{18}$H$_{27}$N$_5$O$_5$; ^{1}H NMR (DMSO-d_6) δ 10.75 (s, 1H, NHOH), 10.0 (br, 3H, NH$_3$ (aryl)), 8.45 (m, 1H, NHBn),

8.10 + 8.25 (m, 1H, NH (Asn)), 6.85–7.45 (2 s, 6H, NH$_2$ (Asn), C$_6$H$_4$), 4.62 (m, 1H, Hα (Asn)), 4,30 (m, 2H, CH$_2$ (Bn)), 3.10–3.20 (2 dd, 1H, H-C2 (Mal)), 2.50 (m, 2H, CH$_2$ (Asn)), 1.40–1.65 (m, 3H, H-C3 (Mal) + H-C4 (Mal)), 0.85 (d, 6H, 2 CH$_3$); diastereomeric ratio, 44:56.

(2R,S)-HONH-Mal(i-Bu)-hPhe-NH-CH$_2$CH$_2$-Ph-(p-Me) (18). To Z-hPhe-OH (160 mg, 0.5 mmol) in THF at 0 °C were added 2-(p-tolyl)ethylamine (68 mg, 0.5 mmol), HOBt (70 mg, 0.5 mmol), and EDCI (100 mg, 0.53 mmol). After 12 h the reaction mixture was diluted with AcOEt and then washed with 5% KHSO$_4$, 5% NaHCO$_3$, and water. The organic layer was dried over MgSO$_4$ and evaporated to dryness: yield 0.2 g (93%); TLC (AcOEt/n-hexane, 2:1) R_f 0.2. Upon hydrogenation in MeOH over Pd/C the resulting H-hPhe-NH-CH$_2$CH$_2$-Phe-(p-Me) was coupled with the malonic acid derivative **2** by the EDCI/HOBt method and worked up as reported for **9**; after hydrogenation the title compound was precipitated from MeOH with n-hexane: yield 70% over the two steps; TLC (CHCl$_3$/MeOH, 9:1) R_f 0.4; FAB-MS m/z 454.2 [M + H$^+$]; M_r = 453.26 calcd for C$_{26}$H$_{35}$N$_3$O$_4$; ^{1}H NMR (DMSO-d_6) δ 10.45 (s, 1H, NHOH), 8.92 (s, 1H, OH), 8.05 (m, 1H, NH-CH$_2$CH$_2$-Ph), 7.80 + 7.95 (2 d, 1H, NH (hPhe)), 7.05–7.30 (m, 9H, C$_6$H$_5$, C$_6$H$_4$), 4.23 (m, 1H, Hα (hPhe)), 3.20–3.40 (m, 2H, NH-CH_2-CH$_2$-Ph), 3.05 + 3.15 (2 dd, 1H, H-C2 (Mal)), 2.45 + 2.68 (2 m, 4H, NH-CH$_2$CH_2-Ph, Hγ (hPhe)), 2.22 (s, 3H, CH$_3$ (aryl)), 1.75 + 1.85 (2 m, 2H, Hβ (hPhe)), 1.45–1.60 (m, 3H, H-C3 (Mal) + H-C4 (Mal)), 0.85 (m, 6H, 2 CH$_3$); diastereomeric ratio, 23:77.

(2R,S)-HONH-Mal(i-Bu)-hPhe-NH-CH$_2$CH$_2$-Ph-(p-OH) (19). Z-hPhe-OH (160 mg, 0.5 mmol) was reacted with tyramine (100 mg, 0.75 mmol), and the reaction mixture was worked up as described for **18**: yield 0.21 g (91%); TLC (CHCl$_3$/MeOH, 9:1) R_f 0.5. Upon hydrogenation in MeOH over Pd/C the resulting H-hPhe-NH-(CH$_2$)$_2$-C$_6$H$_4$-(p-OH) was coupled with **2** by the EDCI/HOBt method and worked up as reported for compound **9**; after hydrogenation the title compound was precipitated from MeOH with n-hexane: yield 81% over the two steps; TLC (CHCl$_3$/MeOH, 9:1) R_f 0.25; FAB-MS m/z 456.1 [M + H$^+$]; M_r = 455.24, calcd for C$_{25}$H$_{33}$N$_3$O$_5$; ^{1}H NMR (DMSO-d_6) δ 10.55 (s, 1H, NHOH), 9.13 (s, 1H, OH (aryl)), 8.92 (s, 1H, OH), 8.05 (m, 1H, NH-CH$_2$CH$_2$-Ph), 7.80 + 7.95 (2 d, 1H, NH (hPhe)), 6.75–7.30 (m, 9H, C$_6$H$_5$ + C$_6$H$_4$), 4.23 (m, 1H, Hα (hPhe)), 3.20–3.40 (m, 2H, NH-CH_2-CH$_2$-Ph), 3.05 + 3.15 (2 dd, 1H, H-C2 (Mal)), 2.45 + 2.68 (2 m, 4H, NH-CH$_2$CH_2-Ph, Hγ (hPhe)), 1.75 + 1.85 (2 m, 2H, Hβ (hPhe)), 1.45–1.60 (m, 3H, H-C3 (Mal) + H-C4 (Mal)), 0.85 (m, 6H, 2 CH$_3$); diastereomeric ratio, 24:76.

(2R,S)-HONH-Mal(i-Bu)-hPhe-NH-CH$_2$CH$_2$-Ph-(p-COOMe) (20). Z-hPhe-OH (160 mg, 0.5 mmol) was reacted with NH$_2$-CH$_2$CH$_2$-Ph-(p-COOMe) (108 mg, 0.75 mmol) under the conditions described for **18**: yield 170 mg (72%); TLC (AcOEt/n-hexane, 2:1) R_f 0.35. Upon hydrogenation the resulting H-hPhe-NH-CH$_2$CH$_2$-Ph(p-COOMe) was coupled with **2** by the EDCI/HOBt method, and the reaction mixture was worked up as reported for the Ala analogue **9**; after hydrogenation the title compound was precipitated from MeOH with n-hexane: yield 63% over the two steps; TLC (CHCl$_3$/MeOH, 9:1) R_f 0.4; FAB-MS m/z 498.4 [M + H$^+$]; M_r = 497.25 calcd for C$_{27}$H$_{35}$N$_3$O$_6$; ^{1}H NMR (DMSO-d_6) δ 10.58 (s, 1H, NHOH), 8.98 (s, 1H, OH), 8.15 (m, 1H, NH-CH$_2$CH$_2$-Ph), 7.95 + 8.05 (2 d, 1H, NH (hPhe)), 7.00–7.80 (m, 9H, C$_6$H$_5$ + C$_6$H$_4$), 4.23 (m, 1H, Hα (Phe), 3.80 (s, 3H, COOCH$_3$), 3.20–3.40 (m, 2H, NH-CH_2CH$_2$-Ph), 3.05 + 3.15 (2 dd, 1H, H-C2 (Mal)), 2.45 + 2.80 (2 m, 4H, NH-CH$_2$CH_2-Ph, Hγ (hPhe)), 1.75 + 1.85 (2 m, 2H, Hβ (hPhe)), 1.45–1.60 (m, 3H, H-C3 (Mal) + H-C4 (Mal)), 0.85 (m, 6H, 2 CH$_3$); diastereomeric ratio, 22:78.

(2R,S)-HONH-Mal(i-Bu)-hPhe-NH-CH$_2$CH$_2$-Ph-(p-COOH) (21). Compound **20** (50 mg, 0.1 mmol) was saponified with 1 N NaOH (1 mL) in THF and then diluted with MeOH. The reaction mixture was treated with amberlyst 15 (H$^+$-form) and evaporated to a small volume, and the product was precipitated with ether: yield 30 mg (60%); TLC (CHCl$_3$/MeOH, 4:1) R_f 0.4; FAB-MS m/z 484.2 [M + H$^+$]; M_r = 483.24 calcd for C$_{26}$H$_{33}$N$_3$O$_6$; ^{1}H NMR (DMSO-d_6) δ 10.56 + 10.53 (2

s, 1H, NH*OH*), 8.98 (br, 1H, OH), 8.15 (m, 1H, N*H*-CH₂CH₂-Ph), 7.95 (d, 1H, NH (*h*Phe)), 7.00−7.90 (m, 9H, C₆H₅ + C₆H₄), 4.23 (m, 1H, Hα (hPhe), 3.20−3.40 (m, 2H, NH-C*H₂*CH₂-Ph), 3.05 + 3.15 (2 dd, 1H, H-C2 (Mal)), 2.45 + 2.80 (2 m, 4H, NH-CH₂C*H₂*-Ph, Hγ (*h*Phe)), 1.75 + 1.85 (2 m, 2H, Hβ (*h*Phe)), 1.45−1.60 (m, 3H, H-C3 (Mal) + H-C4 (Mal)), 0.85 (m, 6H, 2 CH₃); diastereomeric ratio, 50:50.

(2*R,S*)-HONH-Mal(Bn)-*h*Phe-NH-CH₂CH₂-Ph-(*p*-Me) (22). The malonic acid derivative **4** (90 mg, 0.3 mmol) was condensed with H-*h*Phe-NH-CH₂CH₂-Ph-(*p*-Me) (80 mg, 0.2 mmol), and the product was isolated as described for **18**: TLC (CHCl₃/MeOH, 9:1) R_f 0.75. Upon hydrogenation over Pd/C in MeOH the product was precipitated from MeOH with *n*-hexane: yield 41 mg (52%) over the two steps; TLC (CHCl₃/MeOH, 9:1) R_f 0.45; FAB-MS *m/z* 488.2 [M + H⁺]; M_r = 487.24 calcd for C₂₉H₃₃N₃O₄; ¹H NMR (DMSO-*d₆*) δ 10.54 + 10.51(2 s, 1H, N*H*OH), 8.98 (br, 1H, OH), 7.90−8.05 (m, 2H, N*H*-CH₂CH₂-Ph, NH (*h*Phe)), 6.95−7.30 (m, 14H, 2 C₆H₅ + C₆H₄), 4.15 + 4.23 (2 m, 1H, Hα (*h*Phe)), 1.6−3.40 (m, 10H, 5 CH₂), 2.22 (s, 3H, CH₃ (aryl)); diastereomeric ratio, 43:57.

(2*R,S*)-HONH-Mal(CH₂CH₂-Ph)-*h*Phe-NH-CH₂CH₂-Ph-(*p*-Me) (23). The malonic acid derivative **6** (95 mg, 0.3 mmol) was reacted with H-*h*Phe-NH-CH₂CH₂-Ph-(*p*-Me) (130 mg, 0.3 mmol) as described for **18**. Upon hydrogenation, the product was precipitated from MeOH with *n*-hexane: yield 81 mg (72%) over the two steps; TLC (CHCl₃/MeOH, 9:1) R_f 0.4; FAB-MS *m/z* 502.1 [M + H⁺]; M_r = 501.24 calcd for C₃₀H₃₅N₃O₄; ¹H NMR (DMSO-*d₆*) δ 10.54 + 10.51 (2 s, 1H, N*H*OH), 8.98 (s, 1H, OH), 7.90−8.05 (m, 2H, N*H*-CH₂CH₂-Ph, NH (*h*Phe)), 7.00−7.35 (m, 14H, 2 C₆H₅ + C₆H₄), 4.23 (m, 1H, Hα (hPhe)), 1.6−3.40 (m, 12H, 6 CH₂), 2.22 (s, 3H, CH₃ (aryl)); diastereomeric ratio, 25:75.

(2*R,S*)-HONH-Mal(OH)-*h*Phe-NH-CH₂CH₂-Ph-(*p*-Me) (24). The malonic acid derivative **7** (105 mg, 0.33 mmol) was reacted with H-*h*Phe-NH-CH₂CH₂-Ph-(*p*-Me) (172 mg, 0.4 mmol) under the conditions described for **18**. After hydrogenolysis of both *O*-benzyl groups over Pd/C, the product was precipitated from MeOH with *n*-hexane: yield 110 mg (53%) over the two steps; TLC (CHCl₃/MeOH, 9:1) R_f 0.2; FAB-MS *m/z* 414.0 [M + H⁺]; M_r = 413.19 calcd for C₂₂H₂₇N₃O₅; ¹H NMR (DMSO-*d₆*) δ 10.70 (s, 1H, N*H*OH), 8.12 + 8.05 (2 dd, 1H, N*H*-CH₂CH₂-Ph), 7.95 (d, 1H, NH (*h*Phe)), 7.00−7.35 (m, 9H, C₆H₅ + C₆H₄), 4.38 (s, 1H, H-C2 (Mal)), 4.28 (m, 1H, Hα (*h*Phe), 1.6−3.40 (m, 8H, 4 CH₂), 2.22 (s, 3H, CH₃ (aryl)); diastereomeric ratio, 45:55.

(2*R,S*)-HONH-Mal(*i*-Bu)-OEt (25). Compound **1** (0.59 g, 2 mmol) was hydrogenated in MeOH over 10% Pd/C: yield 390 mg (95%) of colorless crystals; TLC (CHCl₃/MeOH, 9:1) R_f 0.4; FAB-MS *m/z* 204.1 [M + H⁺]; M_r = 203.15 calcd for C₉H₁₇NO₄; ¹H NMR (DMSO-*d₆*) δ 10.70 (s, 1H, N*H*OH), 8.95 (s, 1H, OH), 4.05 (m, 2H, C*H₂*CH₃), 3.13 (dd, 1H, H-C₂ (Mal)), 1.4−1.7 (m, 3H, H-C3 (Mal), H-C4 (Mal)), 1.15 (t, 3H, CH₂C*H₃*(Et)), 0.83 (d, 6H, 2 CH₃ (Mal)).

(2*R,S*)-HONH-Mal(Ph)-OEt (26). (2*R,S*)-BnONH-Mal-(Ph)-OEt was prepared as described for **1** from (2*R,S*)-EtO-Mal(Ph)-OK³⁴ and then hydrogenated in MeOH over Pd/C: yield 82%; TLC (AcOEt/*n*-hexane, 1:1) R_f 0.15; FAB-MS *m/z* 224.2 [M + H⁺]; M_r = 223.1 calcd for C₁₁H₁₃NO₄; ¹H NMR (DMSO-*d₆*) δ 10.70 (s, 1H, N*H*OH), 9.00 (s, 1H, OH), 7.15−7.32 (m, 5H, C₆H₅), 4.05−4.15 (m, 2H, C*H₂*CH₃), 3.10 (dd, 1H, H-C2 (Mal)), 1.18 (t, 3H, CH₂C*H₃*).

(2*R,S*)-HONH-Mal(Bn)-OEt (27). Compound **3** (165 mg, 0.5 mmol) was hydrogenated in MeOH over 10% Pd/C: yield 86 mg, 72%; TLC (AcOEt/*n*-hexane, 1:1) R_f 0.15; FAB-MS *m/z* 238.1 [M + H⁺]; M_r = 237.25 calcd for C₁₂H₁₅NO₄; ¹H NMR (DMSO-*d₆*) δ 10.63 (s, 1H, N*H*OH), 8.95 (s, 1H, OH), 7.15−7.30 (m, 5H, C₆H₅), 4.05 (m, 2H, C*H₂*CH₃), 3.13 (dd, 1H, H-C2 (Mal)), 3.08 + 2.97 (2 dd, 2H, C3 (Mal)), 1.15 (t, 3H, CH₂C*H₃*).

(2*R,S*)-HONH-Mal(CH₂CH₂-Phe)-OEt (28). Compound **5** (170 mg, 0.5 mmol) was hydrogenated in MeOH over 10% Pd/C: yield 100 mg (79%); TLC (AcOEt/*n*-hexane, 1:1) R_f 0.10; FAB-MS *m/z* 252.1 [M + H⁺]; M_r = 251.15 calcd for C₁₃H₁₇-NO₄; ¹H NMR (DMSO-*d₆*) δ 10.70 (s, 1H, N*H*OH), 8.95 (s, 1H, NHO*H*), 7.15−7.30 (m, 5H, C₆H₅), 4.10 (m, 2H, C*H₂*CH₃), 3.11

(dd, 1H, H-C2 (Mal)), 2.00 + 2.50 (2 m, 4H, H-C3 (Mal)), H-C4 (Mal), 1.15 (t, 3H, CH₂C*H₃*).

(2*R,S*)-HONH-Mal(Bn)-morpholide (29). (2*R,S*)-BnONH-Mal(Bn)-OH (**4**) was coupled with morpholine by the EDCI/HOBt method, and the crude product was dissolved in AcOEt and washed with 5% KHSO₄, 5% NaHCO₃, and water. The organic phase was dried over MgSO₄ and concentrated to small volume. The product was precipitated with pentane and then hydrogenated in MeOH over 10% Pd/C catalyst. The catalyst was filtered off and the filtrate evaporated to dryness: yield 81% over the two steps; TLC (CHCl₃/MeOH, 9:1) R_f 0.4; FAB-MS *m/z* 279.2 [M + H⁺]; M_r = 278.13 calcd for C₁₄H₁₈N₂O₄; ¹H NMR (DMSO-*d₆*) δ 10.47 (s, 1H, N*H*OH), 8.85 (s, 1H, NHO*H*), 7.15−7.30 (m, 5H, C₆H₅), 3.73 (t, 1H, H-C2 (Mal)), 2.90−3.50 (m, 10H, H-C3 (Mal), CH₂(morpholide)).

(2*R,S*)-HONH-Mal(Bn)-NHBn (30). Compound **4** was converted to the benzyl amide and then deprotected by hydrogenolysis as described for **29**: yield 76% over the two steps; TLC (CHCl₃/MeOH, 9:1) R_f 0.3; FAB-MS *m/z* 299.2 [M + H⁺]; M_r = 298.13 calcd for C₁₇H₁₈N₂O₃; ¹H NMR (DMSO-*d₆*) δ 10.41 (s, 1H, N*H*OH), 8.89 (s, 1H, NHO*H*), 8.17 (dd, 1H, NHBn)), 7.10−7.30 (m, 10H, 2 C₆H₅), 4.30 (dd, 1H, C*H*H (NH-Bn)), 4.20 (dd, 1H, C*H*H (NH-Bn)), 3.33 (t, 1H, H-C2 (Mal)), 3.05 (m, 2H, H-C3 (Mal)).

(2*R,S*)-HONH-Mal(CH₂CH₂-Ph)-NHBn (31). Compound **6** was converted to the benzylamide and deprotected by hydrogenolysis as described for **29**: yield 75% over the two steps; TLC (CHCl₃/MeOH, 9:1) R_f 0.4; mp 159 °C; FAB-MS *m/z* 313.2 [M + H⁺]; M_r = 312.14 calcd for C₁₈H₂₀N₂O₃; ¹H NMR (DMSO-*d₆*) δ 10.47 (s, 1H, N*H*OH), 8.93 (s, 1H, NHO*H*), 8.14 (dd, 1H, NHBn)), 7.13−7.33 (m, 10H, 2 C₆H₅), 4.30 (dd, 1H, C*H*H (NHBn)), 4.28 (dd, 1H, C*H*H (NHBn)), 2.99 (t, 1H, H-C2 (Mal)), 2.49 (t, 2H, H-C4 (Mal)), 2.03 (q, 2H, H-C3 (Mal)).

(2*R,S*)-HONH-Mal(*i*-Bu)-NH-(CH₂)₃-Ph (32). (2*R,S*)-BnONH-Mal(*i*-Bu)-OH (**2**) was converted to the 3-phenylpropylamide and deprotected by hydrogenolysis as described for **29**: yield 62% over the two steps; mp 148 °C; FAB-MS *m/z* 293.2 [M + H⁺]; M_r = 292.17 calcd for C₁₆H₂₄N₂O₃; ¹H NMR (DMSO-*d₆*) δ 10.46 (s, 1H, N*H*OH), 8.86 (s, 1H, NHO*H*), 7.69 (dd, 1H, N*H*-(CH₂)₃-Ph), 7.15−7.30 (m, 5H, C₆H₅), 3.09 (dd, 2H, NH-C*H₂*-CH₂-CH₂-Ph), 3.01 (t, 1H, H-C2 (Mal)), 2.55 (dd, 2H, NH-CH₂-CH₂-C*H₂*-Ph), 1.69 (q, 2H, NH-CH₂-C*H₂*-CH₂-Ph), 1.58 (m, 2H, H-C3 (Mal)), 1.43 (n, 1H, H-C4 (Mal)), 0.86 + 0.84 (2 d, 6H, 2 CH₃).

(2*R,S*)-HONH-Mal(Bn)-NH-(CH₂)₃-Ph (33). (2*R,S*)-BnONH-Mal(Bn)-OH (**4**) was converted to the 3-phenylpropylamide and deprotected by hydrogenolysis as described **29**: yield 60% over the two steps; mp 143 °C; FAB-MS *m/z* 327.3 [M + H⁺]; M_r = 326.16 calcd for C₁₉H₂₂N₂O₃; ¹H NMR (DMSO-*d₆*) δ 10.41 (s, 1H, N*H*OH), 8.87 (s, 1H, NHO*H*), 7.73 (dd, 1H, N*H*-(CH₂)₃-Bn), 7.10−7.30 (m, 10H, 2 C₆H₅), 3.05 (t, 1H, H-C2 (Mal)), 3.04 (m, 4H, NH-C*H₂*-CH₂-CH₂-Ph, H-C3 (Mal)), 2.50 (dd, 2H, NH-CH₂-CH₂-C*H₂*-Ph), 1.71 (q, 2H, NH-CH₂-C*H₂*-CH₂-Ph).

(2*R,S*)-HONH-Mal(CH₂CH₂-Ph)-NH-(CH₂)₃-Ph (34). Compound **6** was condensed with 3-phenylpropylamine and the resulting derivative was deprotected by hydrogenolysis as described for **29**: yield 70% over the two steps; mp 134 °C; FAB-MS *m/z* 341.2 [M + H⁺]; M_r = 340.17 calcd for C₂₀H₂₄N₂O₃; ¹H NMR (DMSO-*d₆*) δ 10.46 (s, 1H, N*H*OH), 8.91 (s, 1H, NHO*H*), 7.72 (dd, 1H, N*H*-(CH₂)₃-Ph), 7.10−7.30 (m, 10H, 2 C₆H₅), 3.09 (dd, 2H, NH-C*H₂*-CH₂-CH₂-Ph), 2.95 (t, 1H, H-C2 (Mal)), 2.58 (t, 1H, H-C4 (Mal)), 2.55 (t, 1H, H-C4 (Mal)), 2.49 (dd, 2H, NH-CH₂-CH₂-C*H₂*-Ph),1.99 (q, 2H, H-C3 (Mal)), 1.71 (q, 2H, NH-CH₂-C*H₂*-CH₂-Ph).

(2*R,S*)-HONH-Mal(OH)-NH-(CH₂)₃-Ph (35). Compound **7** was amidated with 3-phenylpropylamine, and the amide derivative was deprotected by hydrogenolysis as described for **29**: yield 81% over the two steps; mp 82−86 °C; FAB-MS *m/z* 253.1 [M + H⁺]; M_r = 252.11 calcd for C₁₂H₁₆N₂O₄; ¹H NMR (DMSO-*d₆*) δ 10.59 (s, 1H, N*H*OH), 8.91 (s, 1H, NHO*H*), 7.86 (dd, 1H, N*H*-(CH₂)₃-Ph), 7.10−7.30 (m, 5H, C₆H₅), 5.90 (d, 1H, OH), 4.25 (d, 1H, H-C2 (Mal)), 3.11 (q, 2H, NH-C*H₂*-CH₂-CH₂-

Ph), 2.57 (dd, 2H, NH-CH$_2$-CH$_2$-CH_2-Ph), 1.73 (quint, 2H, NH-CH$_2$-CH_2-CH$_2$-Ph).

(2*R,S*)-HONH-Mal(*i*-Bu)-NH-(CH$_2$)$_7$-CH$_3$ (36). Compound **2** was condensed with *n*-octylamine, and the resulting amide was deprotected by hydrogenolysis as described for **29**: yield 68.5%; mp 151 °C; FAB-MS *m*/*z* 287.3 [M + H$^+$]; M_r = 286.22 calcd for C$_{15}$H$_{30}$N$_2$O$_3$; ^{1}H NMR (DMSO-d_6, 400 MHz) δ 10.42 (s, 1H, N*H*OH), 8.86 (s, 1H, NHO*H*), 7.55 (dd, 1H, N*H*-C$_8$H$_{17}$), 3.03 (m, 2H, NH-C*H*$_2$-C$_7$H$_{15}$), 2.95 (t, 1H, H-C2 (Mal)), 1.20–1.70 (m, 15H, 2 H-C3 (Mal), H-C4 (Mal), NH-CH$_2$-C$_6$H$_{12}$-Me)), 0.86 + 0.84 (m, 9H, NH-CH$_2$-C$_6$H$_{12}$-CH_3 + 2 CH$_3$).

Abbreviations: MMP, matrix metalloproteinase; MMP8, human neutrophil collagenase; *h*Phe, L-(2-phenyl)ethylglycine (*homo*-phenylalanine); EDCI, 1-ethyl-3-(3-(dimethylamino)-propyl)carbodiimide hydrochloride; HOBT, 1-hydroxybenzotriazole; Mal(R), 2-substituted malonic acid, R = isobutyl (*i*-Bu), phenyl (Ph), benzyl (Bn).

References

(1) Schwartz, M. A.; Van Wart, H. E. Synthetic Inhibitors of Bacterial and Mammalian Interstitial Collagenases. *Prog. Med. Chem.* **1992**, *29*, 271–334.
(2) Beckett, R. P.; Davidson, A. H.; Drummond, A. H.; Huxley, P.; Whittaker, M. Recent Advances in Matrix Metalloproteinase Inhibitor Research. *Drug Discuss. Today* **1996**, *1*, 16–26.
(3) Hagmann, W. K.; Lark, M. W.; Becker, J. W. Inhibition of Matrix Metalloproteinases. *Annu. Rep. Med. Chem.* **1996**, *31*, 231–240.
(4) Murphy, G. Matrix Metalloproteinases and their Inhibitors. *Acta Orthop. Scand., (Suppl. 266)*, **1995**, *66*, 55–60.
(5) Beckett, R. P. Recent Advances in the Field of Matrix Metalloproteinase Inhibitors. *Exp. Opin. Ther. Pat.* **1996**, *6*, 1305–1315.
(6) Lovejoy, B.; Cleasby, A.; Hassell, A. M.; Longley, K.; Luther, M. A.; Weigl, D.; McGeehan, G.; McElroy, A. B.; Drewry, D.; Lambert, M. H.; Jordan, S. R. Structure of the Catalytic Domain of Fibroblast Collagenase Complexed with an Inhibitor. *Science* **1994**, *263*, 375–377.
(7) Borkakoti, N.; Winkler, F. K.; Williams, D. H.; D'Arcy, A.; Broadhurst, M. J.; Brown, P. A.; Johnson, W. H.; Murray, E. J. Structure of the Catalytic Domain of Human Fibroblast Collagenase Complexed with an Inhibitor. *Nature Struct. Biol.* **1994**, *1*, 106–110.
(8) Stams, T.; Spurlino, J. C.; Smith, D. L.; Wahl, R. C.; Ho, T. F.; Qoronfleh, M. W.; Banks, T. M.; Rubin, B. Structure of Human Neutrophil Collagenase Reveals Large S1' Specificity Pocket. *Nature Struct. Biol.* **1994**, *1*, 119–123.
(9) Bode, W.; Reinemer, P.; Huber, R.; Kleine, T.; Schnierer, S.; Tschesche, H. The X-Ray Crystal Structure of the Catalytic Domain of Human Neutrophil Collagenase Inhibited by a Substrate Analogue Reveals the Essentials for Catalysis and Specificity. *EMBO J.* **1994**, *13*, 1263–1269.
(10) Spurlino, J. C.; Smallwood, A. M.; Carlton, D. D.; Banks, T. M.; Vavra, K. J.; Johnson, J. S.; Cook, E. R.; Falvo, J.; Wahl, R. C.; Pulvino, T. A.; Wendoloski, J. J.; Smith, D. L. 1.56 Å Structure of Mature Truncated Human Fibroblast Collagenase. *Proteins Struct. Funct. Genet.* **1994**, *19*, 98–109.
(11) Grams, F.; Reinemer, P.; Powers, F. C.; Kleine, T.; Pieper, M.; Tschesche, H.; Huber, R.; Bode, W. X-ray Structures of Human Neutrophil Collagenase Complexed with Peptide Hydroxamate and Peptide Thiol Inhibitors. *Eur. J. Biochem.* **1995**, *228*, 830–841.
(12) Reinemer, P.; Grams, F.; Huber, R.; Kleine, T.; Schnierer, S.; Pieper, M.; Tschesche, H.; Bode, W. Structural Implications for the Role of the N-Terminus in the "Superactivation" of Collagenases. *FEBS Lett.* **1994**, *338*, 227–233.
(13) Gooley, P. R.; O'Connell, J. F.; Marcy, A. I.; Cuca, G. C.; Salowe, S. P.; Bush, B. L.; Hermes, J. D.; Esser, C. K.; Hagmann, W. K.; Springer, J. P.; Johnson, B. A. The NMR Stucture of the Inhibited Catalytic Domain of Human Stromelysin-1. *Nature Struct. Biol.* **1994**, *1*, 111–118.

(14) Lovejoy, B.; Hassell, A. M.; Luther, A. M.; Weigl, D.; Jordan, S. R. Crystal-Structures of Recombinant 19-kDa Human Fibroblast Collagenase Complexed to Itself. *Biochemistry* **1994**, *33*, 8207–8217.
(15) Grams, F.; Crimmin, M.; Hinnes, P.; Huxley, P.; Pieper, M.; Tschesche, H.; Bode, W. Structure Determination and Analysis of Human Neutrophil Collagenase Complexed with a Hydroxamate Inhibitor. *Biochemistry* **1995**, *34*, 14012–14020.
(16) Van Doren, S. R.; Kurochkin, A. V.; Hu, W. D.; Ye, Q. Z.; Johnson, L. L.; Hupe, D. J.; Zuiderweg, E. R. P. Solution Structure of the Catalytic Domain of Human Stromelysin Complexed with a Hydrophobic Inhibitor. *Protein Sci.* **1995**, *4*, 2487–2498.
(17) Browner, M. F.; Smith, W. W.; Castelhano, A. L. Matrilysin-Inhibitor Complexes: Common Themes among Metalloproteases. *Biochemistry* **1995**, *34*, 6602–6610.
(18) Dhanaraj, V.; Ye, Q.-Z.; Johnson, L. L.; Hupe, D. J.; Ortwine, D. F.; Dunbar, J. B.; Rubin, J. R.; Pavlovsky, A.; Humblet, C.; Blundell, T. L. X-Ray Structure of a Hydroxamate Inhibitor Complex of Stromelysin Catalytic Domain and its Comparison with Members of the Zinc Metalloproteinase Superfamily. *Nature Struct. Biol.* **1996**, *4*, 375–386.
(19) Becker, J. W.; Marcy, A. I.; Rokosz, L. L.; Axel, M. G.; Burbaum, J. J.; Fitzgerald, P. M. D.; Cameron, P. M.; Esser, C. K.; Hagmann, W. K.; Hermes, J. D.; Springer, J. P. Stromelysin-1–3-Dimensional Structure of the Inhibited Catalytic Domain and of the C-Truncated Proenzyme. *Protein Sci.* **1995**, *4*, 1966–1976.
(20) Nishino, N.; Powers, J. C. Peptide Hydroxamic Acids as Inhibitors of Thermolysin. *Biochemistry* **1978**, *17*, 2846–2850.
(21) Johnson, W. H.; Roberts, N. A.; Borkakoti, N. Collagenase Inhibitors: Their Design and Potential Therapeutic Use. *J. Enzymol. Inhib.* **1987**, *2*, 1–22.
(22) Betz, M.; Huxley, P.; Davies, S. J.; Mushtaq, Y.; Pieper, M.; Tschesche, H.; Bode, W.; Gomis-Rüth, F. X. 1.8-Å Crystal Structure of the Catalytic Domain of Human Neutrophil Collagenase (Matrix-Metalloproteinase-8) Complexed with a Peptidomimetic Hydroxamate Primed-Side Inhibitor with a Distinct Selectivity Profile. *Eur. J. Biochem.* **1997**, *247*, 356–363.
(23) Bihovsky, R.; Levinson, B. L.; Loewi, R. C.; Erhardt, P. W.; Polokoff, M. A. Hydroxamic Acids as Potent Inhibitors of Endothelin-Converting Enzyme from Human Bronchiolar Smooth Muscle. *J. Med. Chem.* **1995**, *38*, 2119–2129.
(24) Fournie-Zaluski, M.-C.; Coulaud, A.; Bouboutou, R.; Chaillet, P.; Devin, J.; Waksman, G.; Costentin, J.; Roques, B. P. New Bidantates as Full Inhibitors of Enkephalin-Degrading Enzymes: Synthesis and Analgesic Properties. *J. Med. Chem.* **1985**, *28*, 1158–1168.
(25) Nishino, N.; Powers, J. C. Design of Potent Reversible Inhibitors for Thermolysin. Peptides Containing Zinc Coordinating Ligands and their Use in Affinity Chromatography. *Biochemistry* **1979**, *18*, 4340–4347.
(26) Brandstetter, H.; Engh, R. A.; Graf von Roedern, E.; Moroder, L.; Huber, R.; Bode, W.; Grams, F. Structure of Malonic-Acid–Based Inhibitors Bound to Human Neutrophil Collagenase. *Protein Sci.*, submitted.
(27) Wünsch, E. *Houben-Weyl, Methoden der Organischen Chemie, Synthese von Peptiden*; Springer-Verlag: Stuttgart, 1974; Vols. 15/I and 15/II.
(28) Stack, M. S.; Gray, R. D. Comparison of Vertebrate Collagenase and Gelatinase Using a New Fluorogenic Substrate Peptide. *J. Biol. Chem.* **1989**, *264*, 4277–4281.
(29) Copeland, R. A.; Lombardo, D.; Giannaras, J.; Decicco, C. P. Estimating K_i Values for Tight Binding Inhibitors from Dose Response Plots. *Bioorg. Med. Chem. Lett.* **1995**, *5*, 1947–1952.
(30) Böhm, H. J. LUDI: Rule-Based Automatic Design of New Substituents for Enzyme Inhibitor Leads. *J. Comput.-Aided Mol. Des.* **1992**, *6*, 593–606.
(31) Boettcher, M.; Henklein, P.; Hoffmann, K.; Heder, G.; Siems, W. E.; Niedrich, H. Synthese von N-substituierten Aminosäure-p-nitrobenzylestern als potentielle ACE-Inhibitoren. (Synthesis of N-substituted amino acid p-nitrobenzyl esters as potential ACE-inhibitors.) *Pharmazie* **1986**, *41*, 140.
(32) Hammond, K. M.; Fisher, N.; Morgan, E. N.; Tanner, E. M.; Franklin, C. S. 3: 5-Dioxo-1: 2-diphenylpyrazolidines. The 4-Hydroxy- and Certain 4-Alkoxy- and 4-Alkylamino-Analogues. *J. Chem. Soc.* **1957**, 1062–1067.
(33) Cignarella, G. Synthesis and Configuration of *trans*-1-Amino-4-benzyl-2,6-dimethylpiperazine as an Intermediate of Semisynthetic Rifamycins. *J. Heterocycl. Chem.* **1974**, *11*, 985–988.
(34) Corey, E. J. The Mechanism of the Decarboxylation of αβ- and βγ-Unsaturated Malonic Acid Derivatives. *J. Am. Chem. Soc.* **1952**, *74*, 5897–5905.